JOURNAL OF PROPULSION AND POWER
Vol. 23, No. 4, July–August 2007

Molecular Dynamics Characterization of the Response of Ni/Al Nanolaminates Under Dynamic Loading

Shijin Zhao* and Timothy C. Germann†
Los Alamos National Laboratory, Los Alamos, New Mexico 87545
and
Alejandro Strachan‡
Purdue University, West Lafayette, Indiana 47907

DOI: 10.2514/1.25727

We use a recently developed molecular dynamics method with an accurate, first-principles-based force field to study shock propagation in Ni/Al nanolaminates and the induced (highly exothermic) chemical reactions. We characterize both perfect nanolaminates and specimens containing small (4-nm diameter) voids. The new method enables the accurate description of both the nonequilibrium shock-loading process and the long time evolution of the shocked material, providing an atomic-level picture of the complex interplay between the mechanical, thermal, and chemical processes that govern the behavior of the metastable composites. We shock the nanolaminates in the direction normal to the Ni/Al interfaces, leading to multiple wave reflections, due to the elastic mismatch between Ni and Al; this leads to the Al layers having a higher temperature during the early stages of the process. In the perfect nanolaminates, the chemical reactions start at the interfaces closest to the impact plane and then propagate through the material. A rapid increase in the rate of chemical reactions ($3Ni + Al \rightarrow Ni_3Al$) is observed following the melting of the Ni and Al layers. We estimate the propagation velocity of the chemical front to be about 200 m/s. The porous samples exhibit much faster energy-release rates, due to the mechanical intermixing of Al and Ni caused by shock-induced pore collapse and the higher shock temperatures.

Nomenclature

T = temperature
t = time
u_p = piston velocity

I. Introduction

NANOSTRUCTURED metastable intermolecular composites (MICs) are a relatively new class of materials that can undergo highly exothermic self-sustained chemical reactions and that have a wide range of current and future applications including environmentally benign primers and detonators [1], soldering [2,3], and nanoscale heat sources for biological and chemical neutralization and disease treatment. Nanostructured MICs are composed of solid reactants intermixed at the nanoscale level and exhibit remarkable properties: extremely fast burn rates, high temperatures and power, accompanied by lower volume expansion than in traditional molecular energetic materials with gaseous products. Furthermore, the energy-release rate can be controlled by modifying the nanostructure of the composite [size of particles, porosity, degree of intermixing, and passivation layer (necessary to avoid spontaneous reaction)]; nanostructured MICs can exhibit front-propagation velocities three orders of magnitude faster than their micron-sized counterparts, due to the reduction of the diffusion distances.

Recent experimental work has resulted in tremendous progress toward a more fundamental understanding of the mechanisms that govern the behavior of nanoenergetic materials; for example, the relationship of particle size and combustion velocity [4,5], insight into the dynamic evolution of thermomechanical and chemical processes in metal/metal-oxide composites from spectral emissions [6] and electrical conductivity measurements [7], shock-induced chemistry and ablation of nano-Al-polymer nanocomposited [8], and the role of the passivation layer [9]. Despite such significant progress, several questions remain regarding the underlying molecular-level mechanisms responsible for the unique properties of nanostructured MICs (e.g., the relative role of thermal and mass diffusion, convection, and radiation in reaction-front propagation as a function of nanostructure and composition). In this paper, we use molecular dynamics (MD) to characterize the dynamic loading of Al/Ni nanolaminates (both perfect and with nanopores) and the induced chemical reactions. Our simulations use an accurate first-principles-based atomistic force field to describe the interactions between Ni and Al atoms and provide full atomic-level detail of the loading and response of the material. It is important to stress that in our simulations, we make no approximation regarding the thermal, mechanical, or chemical behavior of the material other than those implicit in the force field description of the atomic interactions, the fact that we are using classical, rather than quantum, dynamics for the atoms (a very good approximation under the conditions of our simulations), and the size of our samples.

The rest of the paper is organized as follows. Section II describes the details of the simulations performed and the details of the nanolaminates characterized. In Sec. III, we address the fast nonequilibrium process of shock loading of the nanolamines, and in Sec. IV. we focus on the chemical reactions that involved longer timescales. Finally, in Sec. V, we summarize our results and draw conclusions.

II. Molecular Dynamics Simulations

A. Overview

We use a recently developed MD technique to model the propagation of a shock wave in perfect and porous Ni/Al nanolaminate specimens and the induced chemical reactions. Our simulation cells contain six Al/Ni bilayers with Ni/Al interfaces normal to the [111] directions of both crystals. The Al and Ni layers are obtained by replicating six-atom face-centered cubic (fcc) cells with axes oriented in the following way: $a = 1/2[\bar{1}\,\bar{1}\,2]$,

Received 8 June 2006; revision received 6 March 2007; accepted for publication 30 March 2007.

*Postdoctoral Scholar, Theoretical Division, Mail Stop G756.
†Technical Staff Member, Applied Physics Division, Mail Stop F663.
‡Assistant Professor of Materials Engineering, 501 Northwestern Avenue; strachan@purdue.edu (Corresponding Author).

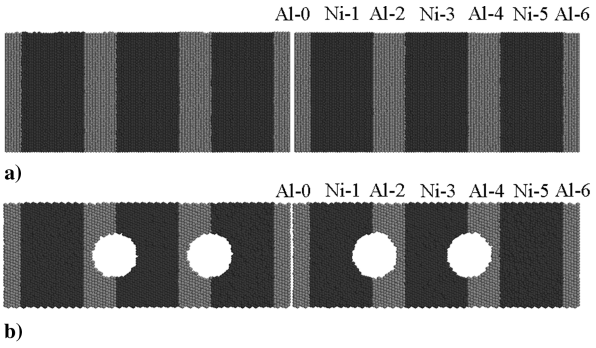

Fig. 1 Snapshots of the initial configurations of a) the perfect nanocomposite and b) the porous nanocomposite.

$b = 1/2[1\bar{1}0]$, and $c = [111]$. Each bilayer contains 15,552 Al and 47,628 Ni atoms, leading to a composition very close to Ni_3Al. Figure 1a shows a snapshot of the perfect Ni/Al nanocomposite; as will be explained in detail later, the central gap in the specimen is used to start the shock waves. As shown in Fig. 1, we start with atomistically sharp interfaces. The degree of interpenetration at the interface, as with many other nano- and microstructural features, is expected to play an important role in the initiation and propagation of the exothermic chemistry: sharp interfaces allow us to focus on the role of voids.

Voids and other defects play a critical role in the initiation of explosives and the propagation of chemical reactions, thus we also studied a porous sample. This defective specimen is obtained from the perfect specimen by cutting four spherical voids, each with a diameter of 40 Å, centered at the Ni/Al interfaces. This size was chosen because it is comparable with that of the laminate periodicity and we expect it to influence the chemical reactions; a systematic study of the role of void size is planned for the future. Figure 1b shows the initial structure of the defective structure in which the four voids can be seen; only a thin slab of the material is shown in Fig. 1b to enable the visualization of the spherical voids.

We describe the atomic interactions via a many-body, embedded-atom, model-type potential parameterized to describe a wide range of ab initio calculations and experimental data of both Ni and Al metals, as well as various alloys including NiAl and Ni_3Al [10]. The potential accurately describes a wide variety of thermal and mechanical properties on Ni/Al systems, including energetics of various crystal structures for Al, Ni, and their alloys, point and planar defects, and the thermal expansion coefficient, an important property in our simulations.

B. MD Simulation of Shock Loading and Long Time Chemistry

Nonequilibrium MD simulations enable a detailed description of the dynamic loading of materials and have provided important information about the induced mechanical response, including plastic deformation [11,12] and structural transitions [13], chemistry and thermal processes in high-energy materials [14] and other molecular systems [15,16], and spall failure [17]. However, nonequilibrium MD simulations of shock loading are limited to relatively short timescales, due to the high velocity of the shock front and the relatively small simulation cells. To characterize longer time-phenomena equilibrium, MD techniques were developed to describe the shocked state of the material [18,19]; however these techniques do not describe the nonequilibrium loading process accurately. In this paper, we use an alternative approach that we recently proposed [20] that combines a realistic description of the nonequilibrium loading process with the ability to characterize long time phenomena (the process of alloying, in our case).

As described earlier, the initial configuration in our simulations consists of a slab containing six Ni/Al bilayers (perfect and porous), with a gap in the central Al layer and three-dimensional periodic boundary conditions. Both specimens are shown in Fig. 1; note that due to the periodicity, our specimen is one slab, not two. Once the system is equilibrated at the desired temperature (300 K in all the simulations in this paper), we add the desired impact velocity to all of the atoms in the system, on top of their thermal velocities. The atoms located to the left of the central gap are assigned a velocity $+u_p$ and the remaining ones are assigned a velocity $-u_p$. To avoid a jump in the velocity field at the cell boundary in the z direction, the upper cell limit is moved with velocity $-u_p$ and the lower limit moves with $+u_p$. When the two Al surfaces collide at the center of the cell, two shock waves will be generated traveling outwards in opposite directions; each shock wave corresponds to a piston velocity. Because our specimens are symmetric with respect to the impact plane (see Fig. 1), the two shock waves will reach the cell boundaries at the same time. At this time, the whole 3-D periodic sample was shocked, and in the case of a homogeneous material, there would be no collective translations in the specimen (the shocked material is at rest in the reference frame of the initial cell). This allows us to explore longer time phenomena; when the two waves meet at the boundary, we stop the compression of the simulation cell and describe the subsequent evolution of the system with constant energy E and volume V MD (NVE ensemble, where N is the number of atoms). The precise time at which the waves meet is determined from the profiles of local velocity across the cell boundary, as will be described elsewhere [21].

To be able to refer to individual layers, we number them starting with the central Al region and moving outwards, as shown in Fig. 1; layers on the left of the shock plane are labeled in the same way as those to the right.

C. Simulation Details and Analysis

In this paper, we report simulations of both perfect and porous nanolaminates that are first equilibrated to $T = 300$ Kand shocked with piston velocities of $u_p = 2$ km/s. We define zero time ($t = 0$) as the transition from the shock regime (compressing boundary conditions) to the constant volume case.

To analyze and characterize the process of shock loading and the subsequent chemical reactions (both spatially), we divide the simulation cells into 59 bins (each bin is about 3 Å thick in the shocked samples) and calculate the properties of each bin as a function of time including composition, center of mass, velocity, and temperature (associated with the kinetic energy of the atoms in each bin calculated after subtracting its center of mass translation).

III. Initial Stage: Nonequilibrium Shock Loading

As a shock wave propagates through the nanolaminate, it generates a sequence of reflected waves that originate from the elastic mismatch between the Al and Ni layers. When a compressive waves travels from Al to Ni, the reflected wave is compressive (because Al is softer than Ni); when a compressive wave travels from Ni to Al, the reflected wave has a tensile character. Thus, the Al layers experience a series of reshocks that lead to significant heating; consequently, during the shock loading and shortly afterwards, the Al regions exhibit higher temperatures than the Ni regions. Figure 2 shows the local temperature as a function of position along the shock direction (z axis) at various times and for the perfect and porous samples characterized. At the beginning of the constant volume stage (see the $t = 0.1$ ps profile in Fig. 2a and the $t = 1$ ps profile in Fig. 2b) the Al slabs are significantly hotter than the Ni slabs; however, this nonequilibrium state is short-lived due to the small thickness of each laminate, and at $t = 10$ ps, the temperature oscillations have decreased significantly, leading to smooth temperature profiles that decrease from the impact plane (center of the cell) to the cell boundaries. Comparing the perfect and defective samples, we note that the central Al layer (Al-0) exhibits similar temperatures in both cases, but the presence of the voids makes the Al-2 and Al-3 layers hotter than in the perfect case; this is also true for the Ni layers. After the large temperature gradients are thermalized, the defective sample exhibits slightly higher local temperatures than the perfect sample.

In addition to temperature, another important difference between the perfect and porous samples is the degree of intermixing between Al and Ni at the end of the shock stage. Figure 3 shows snapshots from our MD simulations at $t = 0$ (the transition between the shock

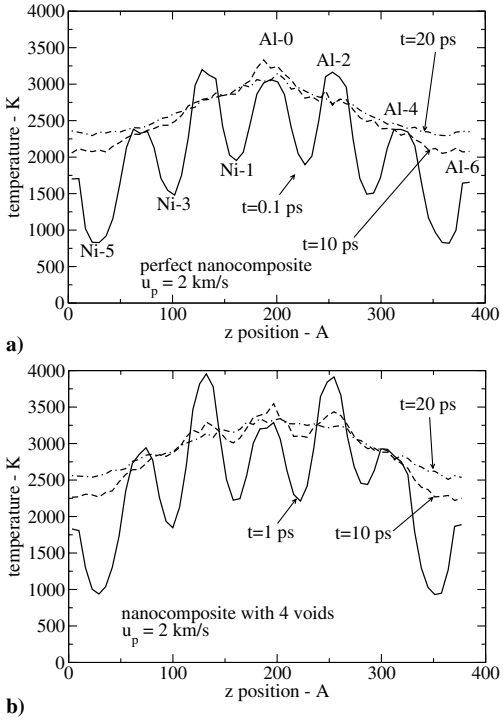

Fig. 2 Temperature profiles at various times for a) the perfect sample and b) the sample with voids. Shock reflections at Ni/Al interfaces lead to increased heating in the Al layers, voids cause a local temperature increase (hot spots).

and constant volume regimes). The perfect sample exhibits rather well-defined Ni/Al interfaces; at this point, the alloying process has just begun. The case of the porous specimen is different: when the shock reaches a void, the atoms near the upstream surface are ejected into the vacuum, when these expanding atoms reach the downstream surface, they recompress and heat up [22]. This process of void collapse not only leads to higher temperatures, but also forces a significant mixing between Ni and Al, increasing the interfacial area. As we will see in the next section, this mechanical mixing speeds up the alloying process significantly.

IV. Late Stage: Chemical Reactions

Figure 4 shows the temporal evolution of the overall temperature of the perfect and porous samples (note that at the early stages, the

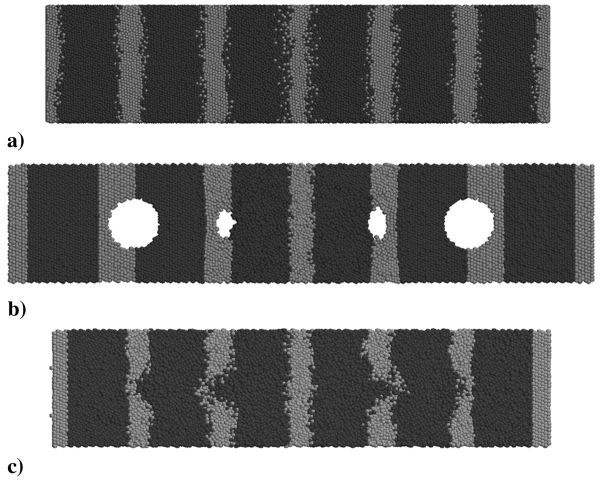

Fig. 3 Snapshots from our MD simulations: a) the perfect sample at $t = 0$ (corresponding to the transition for the shock regime to the constant volume one); b) a porous sample at $t = -2.57$ ps (during the shock compression regime, the collapse of two voids can be seen); and c) a porous sample at $t = 0$ in which the mechanical intermixing of Ni and Al due to void collapse can be observed.

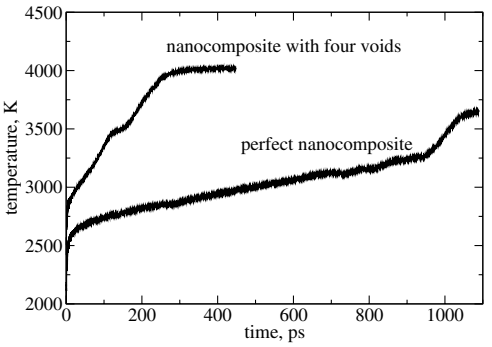

Fig. 4 Temperature as a function of time for the perfect and porous samples; time zero separates the shock and constant volume stages.

system is not in thermodynamic equilibrium and temperature is simply a measure of the kinetic energy of the system). The exothermic alloying process leads to a significant temperature increase in addition to the shock temperature rise; note that the simulations are performed using constant energy and volume MD (NVE ensemble), and so the decrease in potential energy due to the chemical reactions results in an equivalent increase in kinetic energy. This setup mimics the conditions one would expect when analyzing a small region inside a larger material that was shocked, in which the average heat flux to the surroundings would be zero (as in any MD simulations, heat transfer by radiation is neglected). For both the perfect and porous sample, the increase in temperature after the shock compression is similar, about 1680 K for the perfect nanocomposite and 1600 K for the porous case. An important difference between the two samples is much faster reactions for the porous material (over a factor three decrease in reaction timescales). Two factors contribute to this difference: 1) the shock leads to higher temperature in the porous sample compared with the perfect one and 2) void collapse leads to mechanical intermixing of Al and Ni. It is interesting to note that as the reaction progresses, there are a few instances when rate of temperature increase diminishes noticeably (reaching negative values at one point for the perfect sample); this is associated with melting of the Al and Ni layers and will be described in detail next.

The alloying process does not happen simultaneously throughout the composites, and to resolve the chemical reactions both in space and time, we study the temporal evolution of the local composition and temperature for the two specimens. Figure 5 shows the time evolution of the fraction of Al atoms (the ratio between Al atoms and the total number of atoms) at the center of each Al and Ni layer. In the perfect nanocomposite, the chemical reactions start at the interface between the central Al layer (Al-0) and its two neighboring Ni layers (Ni-1). Thus, the fraction of Al atoms in the central bin of the Al-0 layer starts decreasing shortly into the constant volume run; the fraction of Al atoms begins to increase in the center bin of the Ni-1 layers at a longer time (about $t = 220$ ps), due to the larger thickness of the Ni layers. The times of transformation of the layers further away from these central layers are separated by much shorter time intervals, indicating an increase in the propagation velocity of the chemical reaction front. The data for the porous sample shown in Fig. 5b show a different behavior. The Al-2 and Al-4 layers [those immediately downstream from the voids (see Fig. 1b)] start their alloying process at very short times (even at $t = 0$, the fraction of Al atoms is less than one), denoting the mechanical intermixing induced by the shock wave. Overall, the Al-0, Ni-1, and Al-2 layers undergo chemical reaction, with very similar timescales followed by the outer layers. Note that throughout both samples, the Al fraction tends toward 0.25 (i.e., Ni_3Al). A comparison of the radial distribution functions of the reacting system at various times during the evolution with those of equilibrated liquids with the same composition, temperature, and density indicate that the atom structure of the reacting liquids is in local equilibrium [21].

The data in Fig. 5 can be used to locate the propagating chemical reaction front; we define it to be located in the central bin of an Al or Ni layer when their corresponding fractions of Al atoms reach the

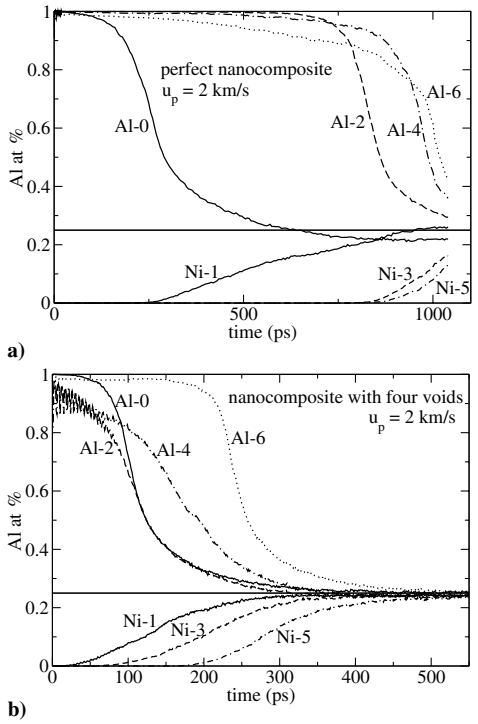

Fig. 5 Temporal evolution of fraction of Al atoms at the center of each Al and Ni layer for a) the perfect sample and b) the porous sample.

midpoint between the initial (1 for Al and 0 for Ni layers) and final values (0.25 in both cases). Figure 6 shows the arrival time of the chemical front as a function of position measured from the impact plane for the perfect nanocomposite. A significant acceleration can be observed after the reaction of the first layers, due to the overall increase in the sample's temperature. From the data in Fig. 6, we can estimate the velocity of the chemical front to be 197 m/s; much larger samples and longer times will be required to obtain a more reliable measure of the front velocity. We are unaware of experiments performed under conditions identical to our simulations that would enable a direct validation of our prediction of the propagation speed. However, propagation velocities were measured in similar materials that indicate that our results fall within very reasonable values. Recent experiments on Pt/Al nanolaminates measured velocities after pulsed laser ignition [5]; the authors found a strong influence of bilayer thickness on propagation velocity (thinner bilayers leading to faster propagation) and velocities ranging from 40 m/s for bilayer thickness of about 975 Å to 70 m/s in the case of 325-Å-thick bilayers. Our result of about 200 m/s for a bilayer thickness of 82.5 Å seems very reasonable. However, in addition to dealing with different materials, there are important differences between our simulations and the experiments: in the experiments, propagation occurred in a direction parallel to the Al/Pt interfaces and in an unshocked material. We are currently performing

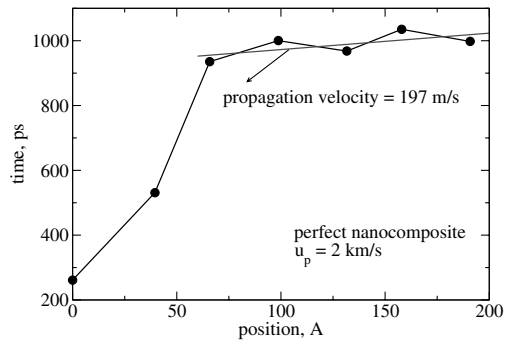

Fig. 6 Arrival time of the chemical front as a function of position measured from the impact plane; the asymptotic velocity is 197 m/s.

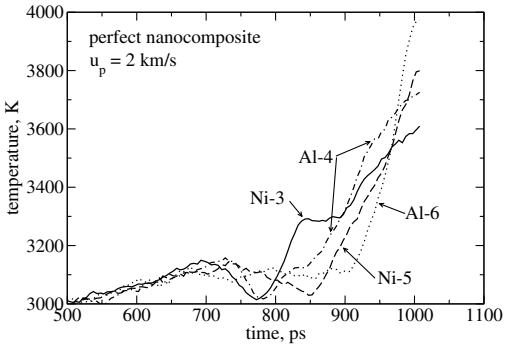

Fig. 7 Local temperature as a function of time for the central bin in various Ni and Al layers for the perfect nanocomposite.

simulations that would reproduce this type of experiments more closely.

To shed light into the propagation mechanisms, it is critical to characterize the events that trigger the alloying process. Thus, we analyzed the time evolution of the local temperature of the sample; Fig. 7 shows the local temperature for the center bin of the layers 3 to 6 for the perfect nanocomposite case as a function of time. We find that melting of the metals precedes the chemical reactions. Melting of layers Ni-3 and Al-4 can be readily seen as a sudden temperature decrease (due to the latent heat of melting) at around $t = 700$ ps; melting is followed by a rapid increase in the local temperature, due to fast alloying triggered by the large mobility of the atoms in the liquid state. Melting of the Ni-5 layer can also be seen, also followed by a large temperature increase. The case of the center of the Al-6 layer is less clear; the local temperature exhibits a long plateau from about $t = 700$ ps until $t = 900$ ps, followed by a very steep increase. The fast temperature increase of the Al-6 layer is likely to be due to the fact that being the last layer to react in a periodic system, it is surrounded by hot, already reacted, material and it does not have to support the reaction of other layers. Melting is responsible for the changes in slope of the overall temperature with time in Fig. 4.

V. Conclusions

In summary, we presented MD simulations of the process of dynamic mechanical loading of Al/Ni metastable nanolaminates and the subsequent induced chemical reactions that transform the reactants (Al and Ni metals) into Ni_3Al. The properties of nanostructured MICs depend strongly not only on composition but also on their nanostructure, and parameters such as porosity play a critical role in their behavior, especially in the energy-release rate (or front-propagation velocity) and initiation. We characterized a nanocomposite consisting of perfect Ni and Al layers and one with porosity: four voids centered at Ni/Al interfaces, each with a diameter of 40 Å. We find that the porous sample exhibits faster chemical reactions that the perfect one due to the mechanical intermixing of Ni and Al caused by the shock-induced void collapse and higher shock temperatures [22]. In the case of the perfect sample, the chemical reactions start at the interfaces closest to the impact planes and propagate outwards; by monitoring the local composition of the sample, we are able follow the propagation of the chemical-reaction front and we estimate its velocity to be around 200 m/s. Under the conditions presented here (i.e., shocks with a piston velocity of 2 km/s), the reaction of Al and Ni is preceded by their melting, which greatly enhances the atomic mobility, leading to a significant increase of the reaction rates.

MD simulations such as the ones presented in this paper have the potential to uncover the fundamental mechanisms that govern the extraordinary properties of nanostructured metastable intermolecular composites. This information is critical to develop physics-based predictive models for this class of energetic material. Such an understanding and predictive tools have the potential to play a critical role in guiding the design of next-generation materials with compositions and nanostructures optimized for specific applications.

Acknowledgments

This work is supported by the Laboratory Directed Research and Development program (project no. LDRD-20050343ER) at Los Alamos National Laboratory, which is operated by the University of California for the U.S. Department of Energy under contract no. W-7405-ENG-36. We thank Yuri Mishin for providing his EAM potential tables.

References

[1] Giles, J. J., "Green Explosives: Collateral Damage," *Nature (London)* Vol. 427, No. 6975, 2004, p. 580.

[2] Swiston, A. J., Jr., Besnoin, E., Duckham, A., Knio, O. M., Weihs, T. P., and Hufnagel, T. C., "Thermal and Microstructural Effects of Welding Metallic Glasses by Self-Propagating Reactions in Multilayer Foils," *Acta Materialia*, Vol. 53, No. 13, 2005, pp. 3713–3719.

[3] Wang, J., Besnoin, E., Duckham, A., Spey, S. J., Reiss, M. E., Knio, O. M., Powers, M., Whitener, M., and Weihs, T. P., "Room-Temperature Soldering with Nanostructured Foils," *Applied Physics Letters*, Vol. 83, No. 19, 2003, pp. 3987–3989.

[4] Bockmon, B. S., Pantoyaa, M. L., Son, S. F., Asay, B. W., and Mang, J. T., "Combustion Velocities and Propagation Mechanisms of Metastable Interstitial Composites," *Journal of Applied Physics*, Vol. 98, No. 6, 2005, pp. 064903-1–064903-7.

[5] Picard, Y. N., Adams, D. P., Palmer, J. A., and Yalisove, S. M., "Pulsed Laser Ignition of Reactive Multilayer Films," *Applied Physics Letters*, Vol. 88, No. 14, 2006, pp. 144102-1–144102-3.

[6] Moore, David, S., Son, Steven, F., and Asay, Blaine, W., "Time-Resolved Spectral Emission of Deflagrating Nano-Al and Nano-MoO 3 Metastable Interstitial Composites," *Propellants, Explosives, Pyrotechnics*, Vol. 29, No. 2, 2004, pp. 106–111.

[7] Tasker, D. G., Asay, B. W., King, J. C., Sanders, V. E., and Son, S. F., "Dynamic Measurements of Electrical Conductivity in Metastable Intermolecular Composites," *Journal of Applied Physics*, Vol. 99, No. 2, 2006, pp. 23705-1–23705-7.

[8] Yang, Y., Wang, S., Sun, Z., and Dlott D., D., "Propagation of Shock-Induced Chemistry in Nanoenergetic Materials: The First Micrometer," *Journal of Applied Physics*, Vol. 95, No. 7, 2004, pp. 3667–3676.

[9] Wang, S., Yang, Y., Yu, H., and Dlott D., D., "Dynamical Effects of the Oxide Layer in Aluminum Nanoenergetic Materials," *Propellants, Explosives, Pyrotechnics*, Vol. 30, No. 2, 2005, pp. 148–155.

[10] Mishin, Y., Mehl, M. J., and Papaconstantopoulos, D. A., "Embedded-Atom Potential for B2-NiAl," *Physical Review B*, Vol. 65, No. 22, 2002, pp. 224114-1–224114-14.

[11] Germann, T. C., Holian, B. L., Lomdahl, P. S., and Ravelo, R., "Orientation Dependence in Molecular Dynamics Simulations of Shocked Single Crystals," *Physical Review Letters*, Vol. 84, No. 23, 2000, pp. 5351–5354.

[12] Kadau, K., Germann, T. C., Lomdahl, P. S., and Holian, B. L., "Atomistic Simulations of Shock-Induced Transformations and Their Orientation Dependence in bcc Fe Single Crystals," *Physical Review B*, Vol. 72, No. 6, 2005, pp. 64120-1–64120-14.

[13] Kadau, K., Germann T. C., Lomdahl P. S., and Holian, B. L., "Microscopic View of Structural Phase Transitions Induced by Shock Waves," *Science*, Vol. 296, No. 5573, 2002, pp. 1681–1684.

[14] Strachan, A., van Duin, A. C. T., Chakraborty, D., Dasgupta, S., and Goddard, W. A., "Shock Waves in High-Energy Materials: The Initial Chemical Events in Nitramine RDX," *Physical Review Letters*, Vol. 91, No. 9, 2003, pp. 098301-1–098301-4.

[15] Elert, M. L., Zybin, S. V., and White, C. T., "Molecular Dynamics Study of Shock-Induced Chemistry in Small Condensed-Phase Hydrocarbons," *Journal of Chemical Physics*, Vol. 118, No. 21, 2003, pp. 9795–9801.

[16] Strachan, A., and Holian, B. L., "Energy Exchange Between Mesoparticles and Their Internal Degrees of Freedom," *Physical Review Letters*, Vol. 94, No. 1, 2005, pp. 014301-1–014301-4.

[17] Strachan, A., Cagin, T., and Goddard, W. A., "Critical Behavior in Spallation Failure of Metals," *Physical Review B*, Vol. 63, No. 6, 2001, pp. 060103-1–060103-4.

[18] Ravelo, R., Holian, B. L., Germann, T. C., and Lomdahl, P. S., "Constant-Stress Hugoniostat Method for Following the Dynamic Evolution of Shocked Matter," *Physical Review B*, Vol. 70, No. 1, 2004, pp. 14103-1–14103-9.

[19] Reed, Evan, J., Fried, Laurence, E., and Joannopoulos, J. D., "A Method for Tractable Dynamic Studies of Single and Double Shock Compression," *Physical Review Letters*, Vol. 90, No. 23, 2003, pp. 235503-1–235503-4.

[20] Zhao, S., Germann, T. C., and Strachan, A., "Molecular Dynamics Simulations of Shock-Induced Chemical, Mechanical, and Thermal Processes in Ni/Al Nanolaminates," *AIP Conference Proceedings*, Vol. 845, No. 1, 2006, pp. 593–596.

[21] Zhao, S., Germann, T. C., and Strachan, A., "Atomistic Simulations of Shock-Induced Alloying Reactions in Ni/Al Nanolaminates," *Journal of Chemical Physics*, Vol. 125, No. 16, 2006, pp. 164707-1–164707-8.

[22] Holian, B. L., Germann, T. C., Maillet, J.-B., and White, C. T., "Atomistic Mechanism for Hot Spot Initiation," *Physical Review Letters*, Vol. 89, No. 28, 2002, pp. 285501-1–285501-4.

S. Son
Associate Editor